

Bulletin of the Seismological Society of America

Vol. 74

October 1984

No. 5

SOURCE PARAMETERS OF TWO $M_L \sim 5$ EARTHQUAKES NEAR ANZA, CALIFORNIA, AND A COMPARISON WITH AN IMPERIAL VALLEY AFTERSHOCK

BY ARTHUR FRANKEL*

ABSTRACT

Strong-motion records were used to determine the seismic moments, source dimensions, and stress drops for two earthquakes near the proposed Anza seismic gap (Thatcher *et al.*, 1975) along the San Jacinto fault: the 25 February 1980 (M_L 5.5) event and the shock of 15 June 1982 (M_L 4.8). Seismic moments determined for the two events were 2.5×10^{23} and 1.1×10^{23} dyne cm, respectively. The source radii were estimated from the displacement pulse widths using the source model of Madariaga (1976). Static stress drops for the 1980 and 1982 earthquakes were calculated as 110 and 100 bars, respectively. Stress drops determined from the rms accelerations using the method of Hanks and McGuire (1981) were 220 bars for the 1980 earthquake and 180 bars for the 1982 event. The long-period seismic moments for these events, derived from regional recordings of 30- to 40-sec Love waves, were a factor of two to three greater than the moments estimated from the strong-motion records.

As a comparison to the Anza events, source parameters were also determined from strong-motion records for an immediate aftershock (M_L 5.0) of the 1979 Imperial Valley earthquake. The seismic moment of this aftershock was calculated as 4.2×10^{23} dyne-cm, and its static stress drop was 130 bars. Static stress drops calculated from the displacement pulse shapes for the three events studied in this paper, as well as for an aftershock of the Oroville earthquake reported by Fletcher *et al.* (1980), exhibit a relatively narrow range between about 100 and 180 bars. This result indicates that the stress drops of the two main shocks near Anza were not unusually high, relative to those of certain aftershocks in other tectonic settings in California.

INTRODUCTION

This paper presents determinations of seismic moment, source dimension, and static stress drop for two main shocks that occurred along the San Jacinto fault system adjacent to the Anza seismic gap proposed by Thatcher *et al.* (1975). The 25 February 1980 event at 10:47 UTC (see Figure 1a) had a local magnitude of 5.5 and a hypocentral depth of 13.6 km, as determined from the Southern California network (SCARLET). The 15 June 1982 shock occurred at 23:49 UTC with a magnitude of 4.8 and depth of 12.2 km. The data for this study consist of records from strong-motion accelerographs (SMAs) from stations less than about 25 km from the events and regional recordings of Love waves at periods of 30 to 40 sec.

Thatcher *et al.* (1975) noted that a 40-km-long segment of the San Jacinto fault was deficient in seismic slip for this century when compared to other segments of

* Present address: Jet Propulsion Laboratory, California Institute of Technology, Pasadena, California 91109.

the fault system. Microearthquake activity appeared to be concentrated at both ends of this segment. From this evidence, Thatcher *et al.* (1980) reasoned that the Anza area was likely to experience a magnitude 6 to 6.5 earthquake in the near future. The 1980 event occurred approximately 5 km south of the southern end of

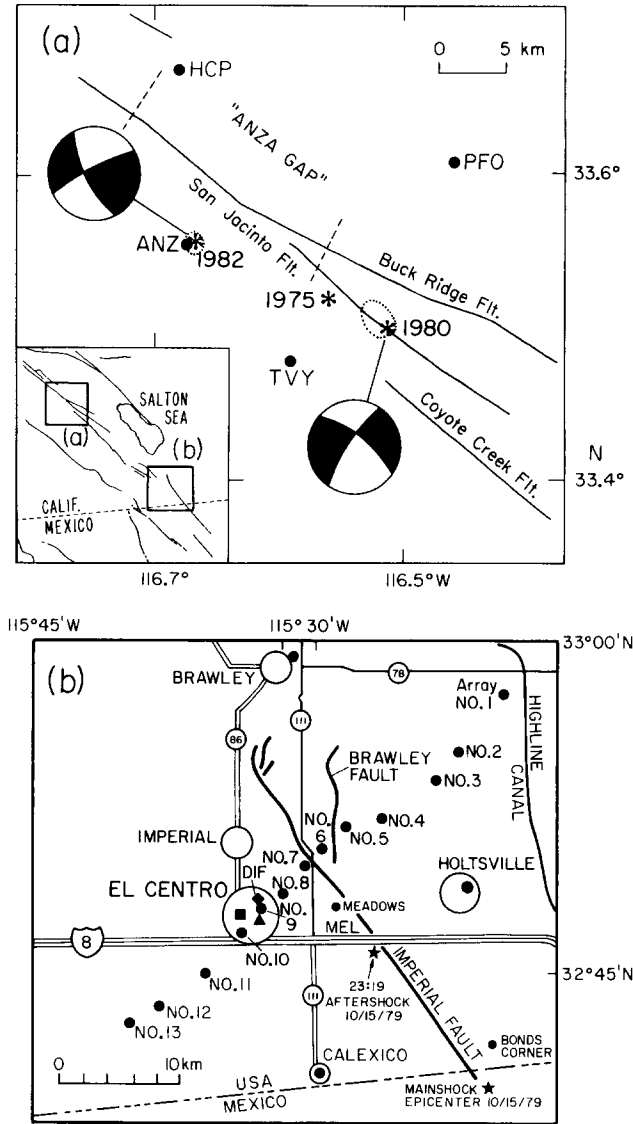


FIG. 1. (a) Map of the area around Anza, California depicting the epicenters of the 1975, 1980, and 1982 earthquakes (asterisks), the SMA sites (circles), and mapped faults (see *inset* for location of map areas). Also indicated are the focal mechanisms of the 1980 (from Given, 1983) and 1982 (D. Given, personal communication, 1983) events on lower hemisphere projections of the focal sphere. The aftershock zones of these events are shown, along with the location of the Anza seismic gap proposed by Thatcher *et al.* (1975). (b) Map of the Imperial Valley area containing the locations of the 1979 Imperial Valley main shock, the 23:19 aftershock studied in this paper and the SMA stations (adapted from Hartzell and Helmberger, 1982).

the seismic gap in an area characterized by high seismicity since at least 1933. The 1982 shock was located about 3 km west of the surface trace of the San Jacinto fault, across from the proposed gap. This event is thought to have occurred off the San Jacinto fault, because microearthquake locations to the north and south of the

gap indicate that the fault dips to the northeast (Sanders and Kanamori, 1984). This study seeks to determine if these two earthquakes had unusually high stress drops, as would be expected if the Anza gap was indeed a locked portion of the San Jacinto fault preparing for a moderate earthquake.

Focal mechanisms for both events reported by Given (1983 and personal communication, 1983) and Sanders and Kanamori (1984) indicate right-lateral, strike-slip faulting on northwest-striking nodal planes. The aftershock zones for these events are shown in Figure 1a, derived from the locations of the southern California network. These zones were determined from aftershocks of magnitude 2 or greater produced within 4 hr of the main shock (location quality A or B). The elongation of both aftershock zones indicates that faulting probably occurred along the northwest striking nodal plane for each event.

A magnitude 4.8 event, the Horse Canyon earthquake, occurred on 2 August 1975 about 5 km northwest of the 1980 event. Strong-motion records and surface waves for this event were analyzed by Hartzell and Brune (1979). They calculated that the long-period moment of this event (30- to 40-sec period) was about five times greater than that calculated from the strong-motion records (1-sec period). They concluded that the rupture began as a high stress drop event on a small asperity and then slowly expanded to a rupture area of 1 km over about 10 sec. We will reevaluate their findings later in this paper, using additional surface wave seismograms.

As a comparison to the Anza events, we determined the source parameters for an immediate aftershock of the 1979 Imperial Valley earthquake (Figure 1b), using strong-motion records. The M_L of this aftershock was 5.0, and its hypocenter was at 9.5 ± 3 km depth (Boore, personal communication). This aftershock occurred only 2.5 min after the main shock. The source process of this event was studied in detail by Liu (1983). The tectonic setting of this event is quite different from that of the Anza events and we might expect its stress drop to be lower. For example, the Imperial Valley has high heat flow (≈ 3 HFU; Combs, 1971), which might reduce the frictional strength of the fault. This contrasts with the much lower values of heat flow, about 1.8 HFU, reported for sites near Anza (Henye and Wasserburg, 1971).

In the following sections, we will first discuss the analysis of the strong-motion records and the regional seismograms of the Anza earthquakes. We then present the results for the Imperial Valley aftershock. We also cite Fletcher *et al.*'s (1980) pulse shape measurements for an aftershock in Oroville, California, as a further comparison with the Anza events. The essential result of this study is that the static stress drops of the Anza events are very similar to the two other earthquakes, despite the difference in the tectonic regimes where they occur.

EVENTS NEAR ANZA

Analysis of strong motion records

Strong-motion records were examined for the stations within 25 km of the Anza events (Figure 1a). The accelerograms for the 1980 event were derived from the phase 1 data supplied by the U.S. Geological Survey (USGS). The phase 1 data consist of unfiltered and unevenly spaced points determined from the photographic records using a laser digitizer. We manually digitized the photographic records for the 1982 event. For all of the earthquakes, the records were detrended, interpolated to a 0.01-sec sampling interval and corrected for instrument response. The resulting accelerograms were rotated into transverse and radial components. A portion of the acceleration record beginning somewhat before the S-wave onset was integrated to

ground velocity and displacement. A cosine taper was applied to the beginning and end (5 per cent of the sample length) of each time series before integration. The integration was accomplished by transforming the waveforms to the frequency domain, dividing by the angular frequency and transforming back to the time domain. A parabolic baseline correction (Nigam and Jennings, 1968) was applied before each successive integration to minimize the long-period error. No filtering was applied to the waveforms in the processing.

Figure 2 depicts the acceleration, velocity, and displacement waveforms for the 1980 event near Anza at the three closest stations: Terwilliger Valley (TVY); Pinyon Flats Observatory (PFO); and Anza Fire Station (ANZ). The transverse components are shown for each station along with the radial component at TVY. A unipolar displacement pulse can be identified at each station. In this paper, we make two measurements of pulse width: the duration τ of the displacement pulse and the time $\tau_{1/2}$ between the onset and the first zero crossing on the velocity waveforms. For

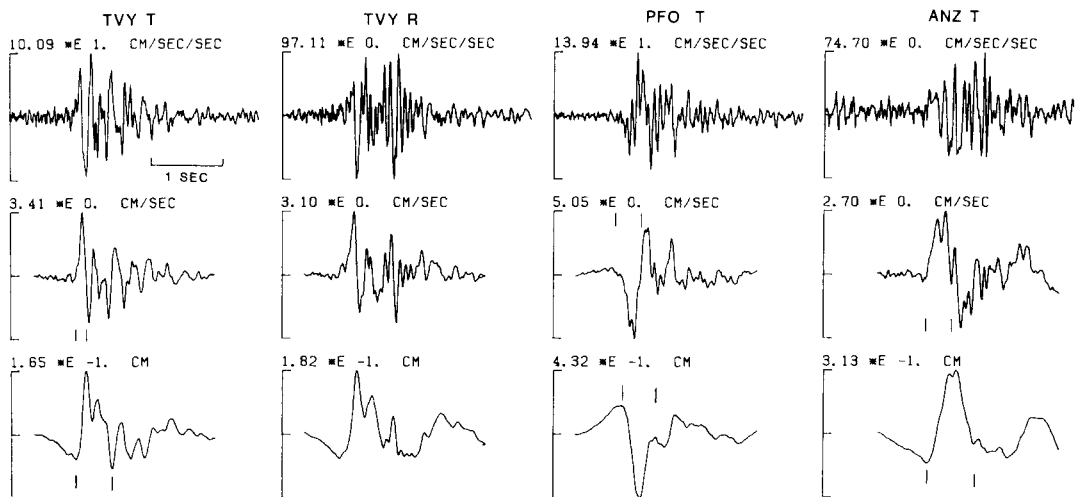


FIG. 2. Acceleration (*top traces*), velocity (*middle*), and displacement (*bottom*) waveforms for the S waves from the 1980 earthquake near Anza. "T" denotes the transverse component and "R" the radial component. Vertical bars indicate our picks for the displacement pulse widths τ and for the velocity pulse half-widths $\tau_{1/2}$. Positive transverse motion is counter-clockwise motion when viewed from above. Positive radial motion is outward from the source. The numbers shown at the top of each plot represent the amplitude between the center and *top* tick marks.

some waveforms, the end of the displacement pulse is difficult to pick because of the arrival of scattered waves. The displacement pulse at PFO (Figure 2) is one such case. In these instances, we extrapolated the initial portion of the back swing of the pulse until it crossed the baseline in order to estimate τ . Our picks for the beginning and end of each displacement pulse are shown in Figure 2. Obviously, the process of determining pulse widths involves some degree of subjectivity.

The source dimension can be estimated from τ or $\tau_{1/2}$ using various types of earthquake source models. Before these measurements can be employed to evaluate source parameters, the effect of the propagation path must be considered. The only path effect we correct for in this analysis is the average, whole path attenuation. We produced an attenuation operator appropriate for each source-receiver distance, assuming a Q of 250. We removed the effect of attenuation on the waveforms by deconvolving the Q operator from the velocity and displacement waveforms. We found that attenuation shortened $\tau_{1/2}$ by a slight amount—at most 0.03 sec. Thus,

whole path attenuation cannot account for the variations in $\tau_{1/2}$ displayed in Figure 2. Values of τ were not measurably changed by the deconvolution.

We have not included the effects of the site response in this study. The site response has been observed to broaden $\tau_{1/2}$ of P -waves by as much as 0.08 sec (Frankel and Kanamori, 1983). The lack of high dynamic range instruments at the SMA sites precluded the determination of the site response using the pulse widths of microearthquakes adjacent to the events of interest. Thus, the pulse widths may be broadened by the site response so that the source radii are overestimated and the stress drops are somewhat underestimated.

We should also note that the stations we examine are close enough to the epicenters relative to the source depth so that the direct S -wave is not contaminated by the head wave or surface waves. For the one radial seismogram used in this study (TVY, 1980 event), the station is less than one source depth from the epicenter. This ensures that the SV wave is incident at a precritical angle and is not distorted.

Some notable features are apparent in the waveforms in Figure 2. $\tau_{1/2}$ is markedly shorter at TVY than for the other two stations. The displacement pulse at ANZ is clearly broader than those at TVY and PFO. Table 1 lists the values of $\tau_{1/2}$ and τ measured from the velocity and displacement waveforms in Figure 2.

TABLE 1
MEASUREMENTS FOR THE EVENTS NEAR ANZA

Component	R (km)	θ ($^{\circ}$)	$\tau_{1/2}$ (sec)	τ (sec)	$R_{\omega\omega}$	Ω_0 (10^{-2} cm—sec)	M_0 (10^{23} dyne—cm)
1980 event							
TVY T	15.5	89	0.15	0.52	0.123	5.69	3.58
TVY R	15.5	89			0.442	6.14	1.97
PFO T	18.9	24	0.35	0.47	0.746	18.30	2.31
ANZ T	21.1	89	0.36	0.65	0.731	15.84	2.28
1982 event							
ANZ E-W	12.2		0.24	0.43	0.42	9.11	1.29
TVY T	16.6	85	0.26	0.45	0.564	8.67	1.27
HCP T	17.5	79		0.67	0.635	7.49	1.03
PFO T	23.5	38	0.35	0.42	0.656	4.18	0.745

Figure 3 contains the acceleration, velocity, and displacement waveforms obtained for the 1982 earthquake. Station ANZ is located essentially directly above this event and both of its components are shown. A plot of the horizontal particle motion of the displacement pulse at ANZ is illustrated in Figure 4. This plot indicates that the S -wave pulse is polarized in the east-west direction. Figure 3 also depicts the ANZ waveforms rotated to coincide with this direction of particle motion. The polarization is not maintained after the direct arrival, producing the relatively prominent, later arrivals on the north-south component. The values of $\tau_{1/2}$ and τ listed in Table 1 were taken from the east-west component, because it has the higher signal to noise ratio and the radiation pattern is better constrained. The latter point will be elaborated later in this section.

Displacement pulse widths τ for the 1982 event were similar at TVY, PFO, and the east-west component of ANZ. The waveform at Hurkey Creek Park (HCP) exhibited a particularly complex character and was not used to determine source duration. $\tau_{1/2}$ was much larger at PFO than at the other stations. In fact, both τ and $\tau_{1/2}$ were remarkably similar at PFO for the 1980 and 1982 events. In contrast,

the values of τ and $\tau_{1/2}$ were significantly larger at ANZ for the 1980 event than the 1982 shock.

The determination of source dimension from the pulse widths presents a major difficulty in this analysis because of the variability in the pulse widths between stations for a given event and the lack of azimuthal coverage required to constrain the rupture geometry. Boatwright (1980a) presented formulas relating $\tau_{1/2}$ to rupture dimension, assuming a particular class of source models. These models characterize

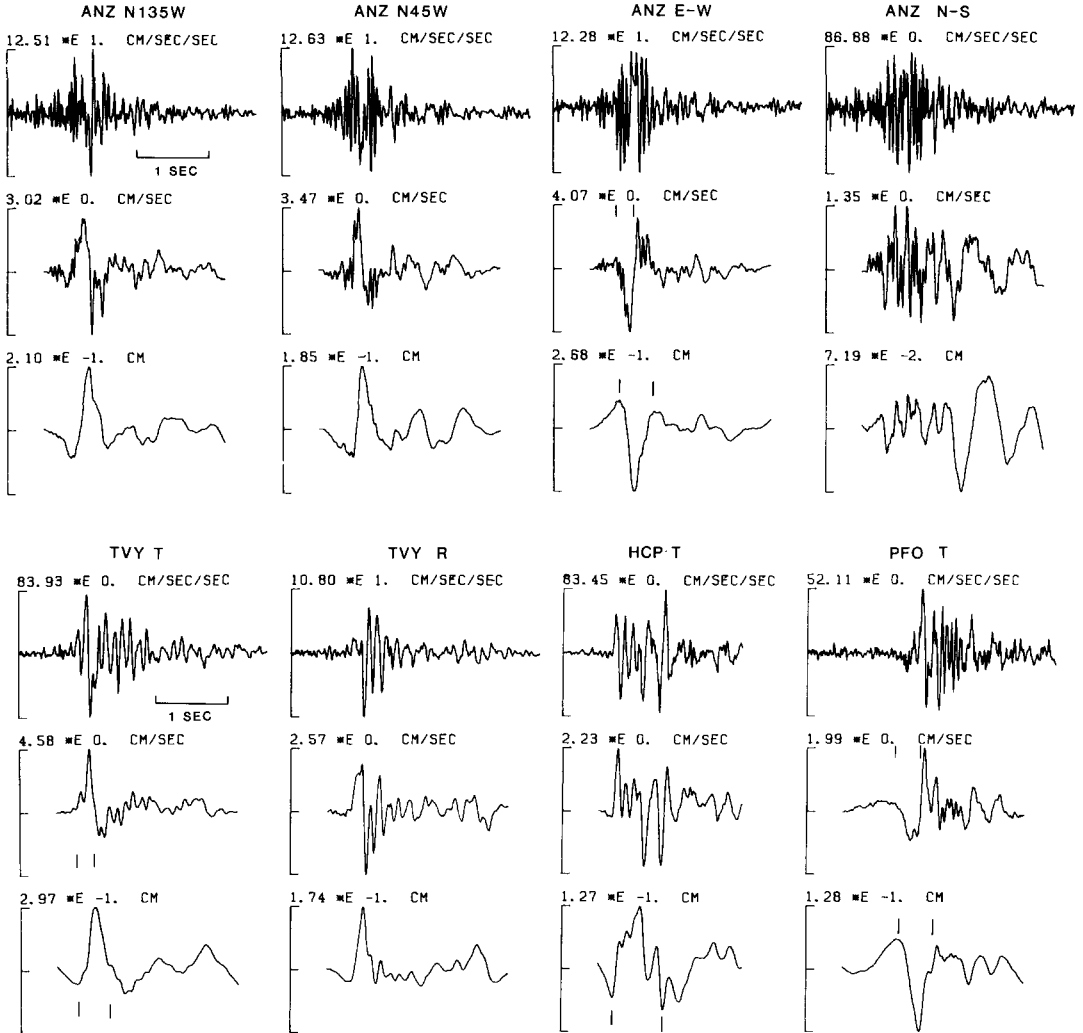


FIG. 3. Acceleration (*top*), velocity (*middle*), and displacement (*bottom*) waveforms for the *S* waves of the 1982 event near Anza. For station ANZ, we show the unrotated components as well as the waveforms rotated both parallel (east-west) and perpendicular (north-south) to the polarization direction.

rupture as nucleating at a point and expanding outward in a circular or elliptical front with a constant rupture velocity and stress drop. In one of these models, first presented by Madariaga (1976), the rupture stops suddenly at the perimeter and a healing phase propagates inward to halt the entire rupture. For circular, subsonic ruptures, these models predict that $\tau_{1/2}$ should be relatively short for body waves which leave the source at small angles to the fault plane. The angle between the ray and the normal to the fault plane is denoted as θ and is listed in Table 1 for the

stations recording the 1980 and 1982 events. The parameters shown in Table 1 indicate that $\tau_{1/2}$ is not a function of θ for the 1980 event. The data for the 1982 shock are not sufficient to draw conclusions about the source geometry. For the 1980 event, these findings imply that either a circular source model is not appropriate for this event or that unaccounted path effects are distorting the values of $\tau_{1/2}$.

The relatively short value of $\tau_{1/2}$ at TVY for the 1980 shock may be a result of unilateral rupture toward that station. Aftershocks of this event extend both to the northwest and updip of the hypocenter (see Figure 1a and Sanders and Kanamori, 1984). A unilateral rupture would produce the smallest values of $\tau_{1/2}$ at rays which leave the source parallel to the direction of rupture propagation (Ben-Menahem, 1962). If the main shock ruptured in a directly nearly updip of the hypocenter, we would expect $\tau_{1/2}$ to be shorter at TVY than at PFO and ANZ. The aftershock distribution is such that one might expect ANZ to have the smallest value of $\tau_{1/2}$, which is not observed. The azimuthal coverage of the strong-motion instruments is too limited to make any conclusions about the rupture geometry of this event.

Our goal in this paper is to compare the gross source parameters (total faulting

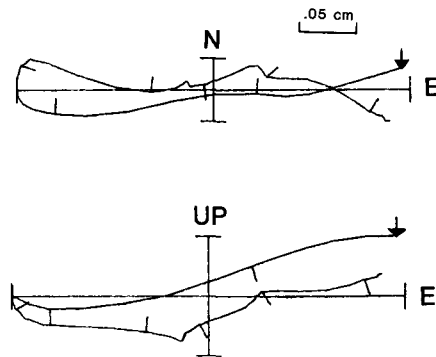


FIG. 4. (Top) Horizontal particle motion of the S -wave displacement pulse at ANZ for the 1982 earthquake. The beginning of each plot is indicated by the arrows. Tick marks are placed every five samples (0.05 sec). Note that the pulse is polarized in the east-west direction. (Bottom) Plot of east-west displacement against vertical displacement for the S -wave pulse at ANZ.

duration, seismic moment, stress drop) of these events. In this paper, we calculate the fault radii from the displacement pulse widths τ . Generally, τ is less variable among the stations for each of the Anza events than in $\tau_{1/2}$ (see Table 1). We use a relationship between radius and pulse width derived from the dynamic source model of Madariaga (1976). Figure 9 in Madariaga (1976) shows synthetic pulse shapes for a circular rupture with a velocity of 0.9 times the shear velocity β . For most takeoff angles θ , the pulse width is approximately equal to $2r/\beta$. Therefore, we calculate r from τ using

$$r = \beta\tau/2. \quad (1)$$

This relationship would vary for different rupture velocities (see Boatwright, 1980a). Other source models would yield different proportionalities between pulse width and radius (see Brune, 1970; Boatwright, 1980a). The uncertainty in the proportionality implies that the absolute values of stress drop derived in this paper may be inaccurate. However, the relative values of static stress drop determined from

the pulse widths are unaffected by this proportionality and, thus, are reliably determined.

Another important caveat is that stress drop measurements made from the pulse widths may not be comparable in their absolute values to those made from the corner frequencies of the displacement spectra. The proportionality between corner frequency and pulse width is sensitive to the shape of the pulse. Commonly, the observed pulse shape differs from the theoretical one, so that corner frequency measurements would produce different stress drops than the pulse widths, even when the same source model is used (see also, Fletcher *et al.*, 1980).

The seismic moments of these events were estimated from the area under their displacement pulses. A flat base line was used when calculating the area. The area was calculated between the beginning and end points of the pulse that were chosen for the determination of source duration. The displacement waveforms were deconvolved with the appropriate attenuation operator before the area was calculated. The area of the pulses corrected for attenuation were, at most, about 10 per cent greater than that of the original pulses. The seismic moment M_0 was calculated from the displacement pulse area Ω_0 by (see, Aki and Richards, 1980)

$$M_0 = \frac{4\pi (\beta_r \rho_r \rho_s)^{1/2} R \beta_s^{5/2} \Omega_0}{FR_{\theta\phi}}. \quad (2)$$

In this equation, ρ denotes density, F is the free surface correction, $R_{\theta\phi}$ is the radiation pattern, and R is the hypocentral distance. The subscripts s and r indicate that the density and shear wave velocity are evaluated at the source and receiver, respectively. For the Anza events, the shear wave velocity was taken to be 3.65 km/sec at the source and 3.1 km/sec at the surface. Density at the source was assigned as 2.7 gm/cm³ and at the receiver was 2.6 gm/cm³. Once the source radius and seismic moment were determined for each event, the static stress drop $\Delta\sigma$ was estimated from the formula for a circular fault given by Brune (1970)

$$\Delta\sigma = \frac{7}{16} \frac{M_0}{r^3}. \quad (3)$$

The waveforms recorded at ANZ for the 1982 event were particularly interesting and they presented difficulties during analysis. The hypocenter calculated for this event by the southern California array is essentially directly beneath the SMA site. An S -wave node for this event occurs near the center of the focal sphere (Figure 1a), close to the expected take-off angle for ANZ. Thus, small errors in the epicentral location of the event can produce large uncertainties in the radiation pattern coefficient calculated for ANZ.

The particle motion of the S -wave displacement pulse provided some constraint on the location of the epicenter relative to station ANZ and hence on the radiation pattern coefficient for the S -wave at ANZ. Figure 4 depicts the east-west displacement plotted against the vertical displacement. Since the S -wave particle motion is perpendicular to the propagation direction, Figure 4 indicates that the range of possible azimuths of the earthquake from the station was 0° (due north) clockwise to 180° (due south). This finding confirms that the ray going towards ANZ is not near the S -wave node of the focal mechanism shown in Figure 1a. The focal mechanism for this shock (Figure 1a) was used to calculate the radiation patterns for the north-south and east-west components in a sector of the focal sphere defined

by angles of incidence between 160° and 180° (from downward vertical) and azimuths from 180° to 360° . This search confirmed that, when the east-west component was ten times or more greater in amplitude than the north-south component, the radiation pattern factor of the east-west component varied within a narrow range between 0.35 and 0.48. Therefore, we used the east-west component at ANZ in our measurements of pulse width and area (see Figure 3) and assigned a radiation pattern coefficient of 0.42.

Table 1 lists the pertinent measurements and calculations for seismic moment, source radius and stress drop. We determined the fault radii from the average pulse width. The stress drop was estimated from the average value of seismic moment and the fault radius. These results are summarized in Table 2. The seismic moment calculated for the 1980 event was $2.5 \pm 0.7 \times 10^{23}$ dyne-cm. This value was averaged from the transverse components at PFO and ANZ and from both the transverse and radial components at TVY. The two components at TVY were averaged into one reading because the transverse component was calculated to be nodal. We obtained a stress drop of 110 bars for the 1980 event. The seismic moment of the 1980 shock was averaged from the transverse components at TVY, HCP, and PFO for the east-west component of ANZ. The calculated value was $1.1 \pm 0.3 \times 10^{23}$ dyne-cm, yielding a stress drop of 100 bars. In a later section, we will compare these

TABLE 2
SUMMARY OF SOURCE PARAMETERS

Event	Pulse Width (sec)	Fault Radius (m)	M_0 ($\times 10^{23}$ dyne-cm)	$\Delta\sigma$ (bars)
25 Feb. 1980 10:47 (Anza)	0.54	990	2.5	110
15 June 1982 23:49 (Anza)	0.43	780	1.1	100
15 Oct. 1979 23:19 (Imperial Valley)	0.62	1130	4.2	130
6 Aug. 1975 3:50 (Oroville)	0.55*	1000	4.0*	180

* Measurements from Fletcher *et al.* (1980).

stress drop estimates with those obtained from the displacement corner frequencies.

We have also determined the static stress drops of these events using the source dimensions estimated from their aftershock zones. The horizontal extent of the aftershock zone of the 1980 shock is about 2.5 km and that of the 1982 event is about 1.4 km (see Figure 1a). We take the locations of the aftershocks occurring within 4 hr of the main shock to define the rupture area. This short length of time was chosen to reduce the possibility of overestimating the fault dimensions, since aftershock zones are often observed to expand with time (see, Given 1983; Corbett and Johnson, 1982). The vertical extent of each aftershock zone is difficult to assess because they are comparable to the uncertainties in the depth determination. Therefore, we assume the rupture zones to be circular and use the horizontal extent of each aftershock zone as the fault diameter.

Table 3 summarizes the calculations of source radius and stress drop derived from the various methods discussed in this paper. The source radii estimated from the aftershock zones are quite similar to the determinations based on pulse widths, especially when considering the uncertainties involved in estimating source radius from pulse width. For the 1980 shock, the pulse widths yield a radius of 990 m, and the aftershock zone is about 1250 m in radius. The pulse widths of the 1982

earthquake indicate a source radius of 780 m, while the aftershock zone is approximately 700 m in radius. The static stress drops calculated from the aftershock zone dimensions and the seismic moments derived from the pulse widths are 56 bars for the 1980 event and 140 bars for the 1982 event. Because of the uncertainties in the relative locations in the aftershocks and the poor constraint on the geometry of the aftershock zones, it is not clear whether this difference in stress drop between these events is significant.

Stress drop from acceleration waveforms

Hanks and McGuire (1981) presented a method of calculating stress drop from the root mean acceleration (a_{rms}). They found that the acceleration spectra for events greater than magnitude 4 could generally be described by a flat portion between the corner frequency f_c at the low-frequency end and a limiting high-frequency denoted as f_{max} . Above f_{max} the spectral amplitude decreases with frequency because of seismic attenuation. The spectral amplitude of the flat portion of the spectrum can be approximately related to a_{rms} by Parseval's theorem. In this manner, Hanks and McGuire (1981) presented a relationship between stress drop and a_{rms}

TABLE 3
SUMMARY OF STRESS DROP DETERMINATIONS FOR THE ANZA
EVENTS

Basis of Determination	Source Model*	1980 Event		1982 Event	
		Radius (m)	Stress Drop (bars)	Radius (m)	Stress Drop (bars)
Pulse width	M	990	110	780	100
Corner frequency	B	800	210	850	78
Aftershock area	—	1250	56	700	140
a_{rms}	B	—	220	—	180

* M = Madariaga (1976) model; B = Brune (1970) model.

such that

$$\Delta\sigma = 3.16\rho Ra_{rms} \sqrt{\frac{f_c}{f_{max}}}. \quad (4)$$

This formula was derived by using the proportionality between corner frequency and fault radius specified by the Brune (1970) model.

We have measured a_{rms} , f_c , and f_{max} from the acceleration waveforms and spectra for the Anza events. Our purpose was to quantify the high-frequency character of these earthquakes. Figure 5 shows the acceleration spectra of the transverse components and our picks of f_c and f_{max} . The acceleration spectra were taken from the waveforms shown after they were appended with zeroes to make time series 5.12 sec in length. A cosine taper was applied to 5 per cent of the length of the waveform at its beginning and end. a_{rms} was calculated from the accelerograms by

$$a_{rms} = \left\{ \frac{1}{t_2 - t_1} \int_{t_1}^{t_2} a^2(t) dt \right\}^{1/2}. \quad (5)$$

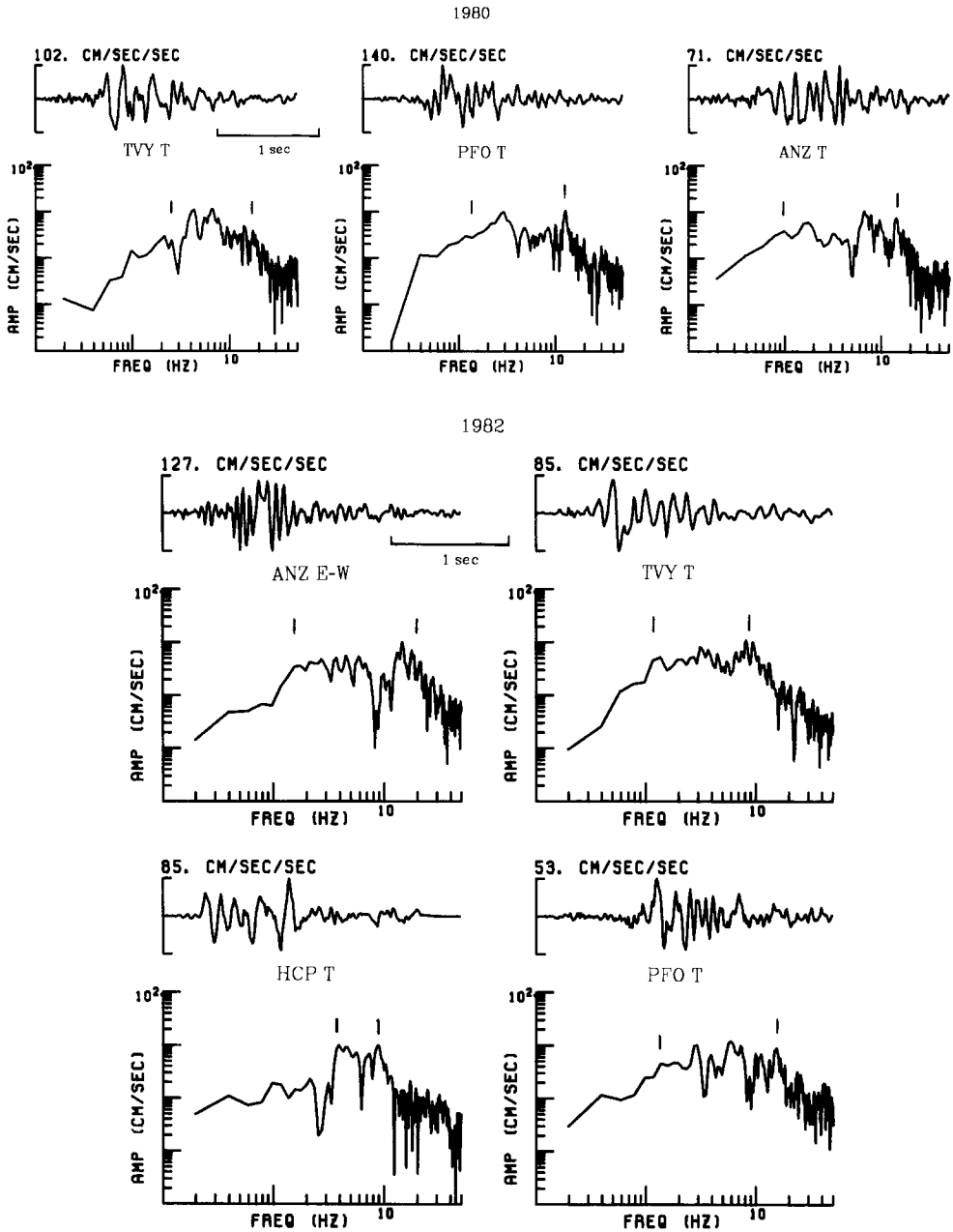


FIG. 5. Acceleration waveforms and spectra for the S waves from the 1980 and 1982 earthquakes. Vertical bars indicate our picks for the corner frequency f_c and f_{max} .

Here t_1 and t_2 were chosen from the beginning and end of the displacement pulses. Values of the parameters calculated from these waveforms and spectra are listed in Table 4.

Several interesting features are apparent in the acceleration spectra of these events (Figure 5). Most of the corner frequencies are between 1 and 2 Hz, although higher corner frequencies are observed at TVY for the 1980 event and at HCP for

the 1982 shock. The corner frequency at HCP is difficult to determine probably because of the complexity of the waveform. Significant differences in f_{\max} are exhibited for stations recording the 1982 event. f_{\max} is 19 Hz at ANZ, 18 Hz at PFO, and only 10 Hz at TVY. For this event, f_{\max} is not a function of source-receiver distance. The ANZ spectrum appears to have a broad spectral peak between 10 and 20 Hz, which may be indicative of a site resonance. The value of f_{\max} is not simply an artifact of local site conditions, because f_{\max} at TVY for the 1980 earthquake is 17 Hz, compared to 10 Hz at TVY for the 1982 shock. Both events are about the same distance from TVY.

The stress drops determined from the a_{rms} values are 220 bars for the 1980 event and 180 bars for the 1982 shock (see Table 4). Hanks and McGuire (1981) reported that values of a_{rms} for California earthquakes are consistent, within a factor of two, with stress drops of 100 bars. They derived stress drops between 80 and 200 bars for seven Oroville aftershocks using their rms accelerations. Thus, the a_{rms} stress drop calculated for the Anza events places them among the highest yet reported using this method.

TABLE 4
MEASUREMENTS FROM THE ACCELERATION
WAVEFORMS AND SPECTRA

Component	f_c (Hz)	f_{\max} (Hz)	a_{rms} cm/sec ²	$\Delta\sigma$ (bars)
1980 event				
TVY T	2.5	17	48.1	244
PFO T	1.6	14	54.4	296
ANZ T	.9	16	28.8	123
Average				220
1982 event				
ANZ E-W	1.8	19	70.8	227
TVY T	1.3	10	39.5	202
HCP T	3.5	9.3	30.9	173
PFO T	1.7	18	17.2	106
Average				180

Stress drops from corner frequencies

So far in this paper we have presented three different sets of stress drop calculations: (1) from the pulse widths and seismic moments using the Madariaga (1976) source model; (2) from the dimensions of the aftershock zones and the seismic moments; and (3) from the rms accelerations using the formula of Hanks and McGuire (1981) based on the source model of Brune (1970). Most measurements of stress drop to date, however, have utilized the corner frequency to determine the fault radius and the relationships given by Brune (1970). The average corner frequency of the 1980 event is 1.7 Hz and that of the 1982 earthquake is 1.6 Hz, excluding HCP which has an anomalous spectral shape (see Table 4). Using the proportionality between corner frequency and fault radius given by Brune (1970), we obtain stress drops of 210 and 78 bars for the 1980 and 1982 earthquakes, respectively (see Table 3). Other measurements of California earthquakes of comparable seismic moments range between about 1 and 200 bars (see Thatcher and Hanks, 1973; Archuleta *et al.*, 1982).

The stress drop calculated for the 1980 event from the corner frequency is higher than the 1982 event largely because of the relatively high corner frequency at TVY for the 1980 earthquake. This high-corner frequency is consistent with the small value of $\tau_{1/2}$ for this waveform, although the total pulse with τ is comparable to those at the other stations. Thus, the stress drop calculations derived from the pulse widths do not exhibit the variation apparent in the estimates made from the corner frequencies.

Surface wave analysis

We analyzed long-period Love waves from the 1980 and 1982 events to estimate their seismic moments at periods of 30 to 40 sec. The seismic moment of a previous event in the area, the Horse Canyon earthquake of 2 August 1975, was also determined. Love waves recorded on stations of the World-Wide Standardized Seismic Network (WWSSN) were digitized for the three events. The SRO station at Albuquerque (AMNO) was used for the 1980 and 1982 earthquakes. The record at the digital WWSSN station at Logmire (LON) was included in the analysis of the 1982 shock. The digitized seismograms were rotated to the transverse direction and compared to synthetic seismograms produced using the method of Harkrider (1964, 1970). The synthetic Love waves were computed with the earth model KHC2 which is tabulated in Hartzell and Brune (1979). The shear wave Q in all the layers was set at 200. A step time function was used for the fault displacement to produce the synthetics.

Figure 6 shows the data and synthesis for the Love waves of the 1975, 1980, and 1982 earthquakes. For the nearer stations, the synthetics match the data fairly well. The agreement degenerates for the more distant stations, although the character of the waveforms are similar. Some stations, such as Berkeley (BKS), exhibit prominent arrivals after the Love wave which are probably caused by multipathing.

The seismic moments for these events were computed by matching the amplitudes of the 30- to 40-sec period Love waves of the data to the synthetics. Love waves in this period range represent the initial half-cycle of the waveforms shown in Figure 6. Table 5 lists the measurements and results. The four stations used for the 1980 event yield a moment of 5.6×10^{23} dyne-cm. The standard deviation for this estimate was unusually large, $\pm 2.6 \times 10^{23}$ dyne-cm, about 50 per cent of the mean. The moment of the 1982 earthquake was determined as $2.3 \pm 0.5 \times 10^{23}$ dyne-cm from four stations. The long-period moments for these two events are about twice those estimated from the strong-motion records. At both long and short periods, the seismic moment of the 1980 event is about 2.5 times that of the 1982 earthquake.

The strong-motion records of the 1975 earthquake were previously analyzed by Hartzell and Brune (1979). They reported a preferred seismic moment from the strong-motion records of 6.5×10^{22} dyne-cm and a long-period moment of 3.0×10^{23} dyne-cm from the Rayleigh waves recorded at Tucson (TUC), a value five times greater than the moment at short-period.

We have determined the long-period moment of the 1975 event to be $1.9 \pm 0.8 \times 10^{23}$ dyne-cm from the Love waves recorded at four stations. This value is two-thirds of the estimate Hartzell and Brune (1979) made from one station. The surface wave moment we calculate is three times that obtained from the strong-motion records by Hartzell and Brune (1979).

To summarize the moment determinations for these events, the moments at periods of 30 to 40 sec are a factor of two to three greater than the moments derived

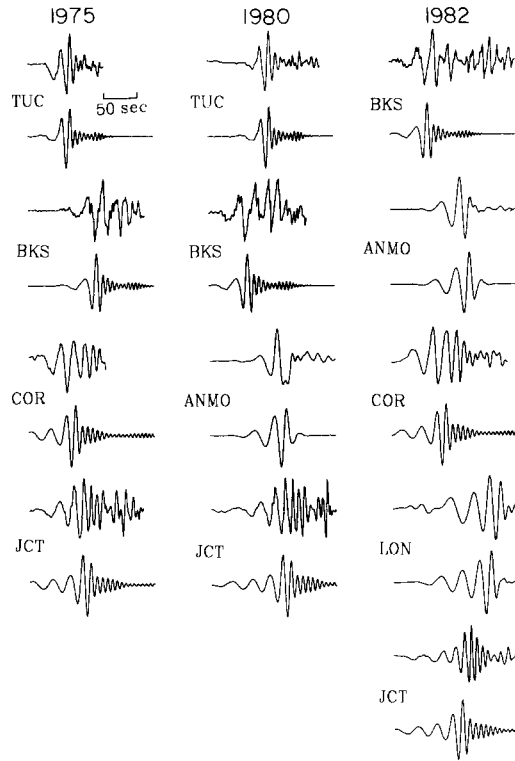


FIG. 6. Love wave data and synthetics for the 1975, 1980, and 1982 events near Anza. For each station, the *upper trace* is the digitized seismogram (rotated to the transverse direction), and the *lower trace* is the synthetic seismogram.

TABLE 5
CALCULATIONS FROM LOVE WAVES

Event	Station	Δ (km)	Moment (10^{23} dyne-cm)
2 Aug. 1975	TUC	557	2.54
	BKS	706	1.08
	COR	1359	2.73
	JCT	1617	1.30
	Average		$1.9 \pm .8$
25 Feb. 1980	TUC	552	2.21
	BKS	711	6.18
	ANMO	939	8.48
	JCT	1612	5.33
	Average		5.6 ± 2.6
15 June 1982	BKS	696	1.60
	ANMO	952	2.08
	COR	1351	2.25
	LON	1528	2.52
	JCT	1628	2.84
	Average		$2.3 \pm .5$

from the strong-motion records at periods of 0.5 to 1 sec. This difference between the long and short-period estimates of moment is typical of those reported in broadband studies of several other earthquakes (see, e.g., Boatwright, 1980b; Wallace *et al.*, 1981). It is generally thought that this discrepancy is caused by the hetero-

geneity along the rupture surface. The short-period moment represents the seismic radiation from localized areas of high strength, whereas the long period energy is produced from a larger portion of the rupture surface.

COMPARISON WITH AN AFTERSHOCK OF THE IMPERIAL VALLEY EARTHQUAKE

For each of the Anza events, the displacement pulse widths exhibited less variation between stations than did the corner frequencies. When the pulse shapes are simple, we would expect that time domain measurements would be more precise than spectral estimates (see, Fletcher *et al.*, 1980). Therefore, as a comparison to the Anza events, we determined the stress drop of an Imperial Valley aftershock using measurements of pulse width and area taken from local strong-motion records.

The aftershock occurred at 23:19 UTC, 2.5 min after the 15 October 1979 Imperial Valley earthquake (see Figure 1b). We derived displacement waveforms in a manner identical to that used for the Anza events. The original data for this processing were the phase 1 accelerograms supplied by the USGS. We have analyzed only the *S* waves for this event, with the goal of estimating its gross source parameters rather than determining a detailed rupture model. Liu (1983) modeled this earthquake as a double event, with the second event about 1 km north of the first one.

The transverse displacement waveforms are shown in Figure 7. Stations AR4, AR9, AR10, and the El Cento differential array were not included in this analysis, because the beginning of the *S*-wave acceleration pulse at these stations had a nodal character. The positions of these nodal stations are consistent with a right-lateral, strike-slip mechanism on a northwest striking nodal plane (see also Liu, 1983). The displacement waveforms for this event are, in general, remarkably simple pulses. The waveforms contain significantly less energy at frequencies greater than 10 Hz than the waveforms of the Anza events. This difference in frequency content is probably caused by the high attenuation thought to occur in the shallow sediments of the Imperial Valley (see Liu, 1983).

Our picks for the duration of the displacement pulses are shown in Figure 7 and listed in Table 6. The widest pulses are observed at Calexico (CLX) and Bonds Corner (BOC), stations which are located to the south of the epicenter. This is consistent with the northward propagating rupture found by Liu (1983). The average pulse width for this event was 0.61 sec. The pulse areas were calculated after deconvolving an attenuation operator corresponding to a *Q* of 250 and a travel time appropriate for each station. We have probably underestimated the attenuation because we have not considered the effects of the shallow, unconsolidated sediments. In using equation (2) to evaluate the seismic moment, we assigned values of 3.2 and 1.1 km/sec for the shear wave velocities at the source and receiver, respectively. These velocities were derived from the *P*-wave values reported by Fuis *et al.* (1983), by assuming a V_p/V_s ratio of $\sqrt{3}$. Densities at the source and receiver were set at 2.7 and 2.3 gm/cm², respectively, following Fuis *et al.* (1983).

Measurements from the waveforms for this event are listed in Table 6 and the source parameters are presented in Table 2. We obtained a seismic moment of 4.2×10^{23} dyne-cm from the average of 10 stations. The surface wave moment of this event could not be computed, because the main shock waveforms obscured the surface waves of this event. The stress drop calculated for this event was 130 bars. It should be noted that the stress drop of this event may be underestimated since the pulses may be significantly broadened by attenuation in the shallow sediments. The stress drop of this shock is remarkably similar to those calculated for the two Anza events (110 and 100 bars, see Table 2).

We did not calculate an a_{rms} stress drop for this event because of the shapes of its acceleration spectra. The spectra were often peaked around the corner frequency, rather than having a flat portion between the corner frequency and f_{max} . Thus, determinations of a_{rms} stress drop for this event using equation (4) would not be directly comparable to the Anza events.

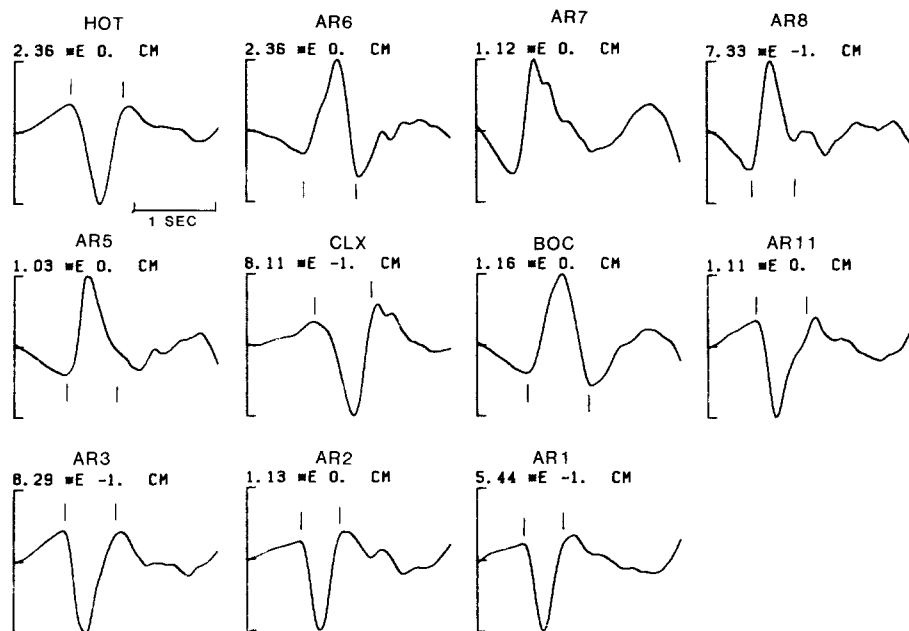


FIG. 7. Transverse displacement pulses for the S waves of the Imperial Valley aftershock of 23:19 UTC. Vertical bars indicate the picks for the pulse durations.

TABLE 6
MEASUREMENTS FOR THE 23:19 UTC IMPERIAL VALLEY
AFTERSHOCK

Station	R (km)	τ (sec)	R_{sp}	Ω_0 (10^{-2} cm—sec)	M_0 (10^{23} dyne—cm)
HOT	12.3	0.65	0.745	111	5.46
AR6	13.0	0.65	0.775	107	5.37
AR8	13.7	0.53	0.555	35.4	2.62
AR5	13.9	0.65	0.583	50.1	3.58
CLX	15.2	0.76	0.442	36.1	3.73
BOC	15.9	0.75	0.794	66.1	3.98
AR11	17.3	0.60	0.460	48.5	5.47
AR3	17.9	0.64	0.464	41.1	4.76
AR2	20.4	0.50	0.446	37.9	5.19
AR1	26.1	0.50	0.600	17.8	2.32

DISCUSSION

Figure 8 shows a graph of the average pulse width plotted against seismic moment for the three events studied in this paper. The seismic moments were taken from the results of the strong-motion analysis. We have also included on this graph a data point representing the parameters of a M_L 4.7 aftershock (3:50 UTC, 6 August

1975) of the Oroville, California earthquake. The average pulse width and seismic moment for this aftershock were taken from Fletcher *et al.* (1980), who analyzed strong-motion records of 10 stations within 15 km of this event. The Oroville earthquakes occurred along the western edge of the Sierra Nevada mountains. Fletcher *et al.* (1980) determined a normal faulting mechanism for this aftershock. We used the seismic moment of 4.0×10^{23} dyne-cm calculated by Fletcher *et al.*, and we averaged the displacement pulse widths they measured for nine of the stations (excluding station 9). The stress drop we computed for this event from the average pulse width and seismic moment was 180 bars. It should be noted that the a_{rms} stress drop reported for this event by Hanks and McGuire (1981) was 173 bars, similar to those of the Anza earthquakes.

The major conclusion of this paper is illustrated in Figure 8: the four earthquakes discussed here display only a factor of two variation in static stress drop, despite the dissimilar tectonic regimes in which they occur. Given the uncertainties in the determination of pulse width and seismic moment, this factor of two variation does not appear to be significant. Errors in the pulse width estimates arise from scattered waves obscuring the true pulse duration and from path effects such as the site

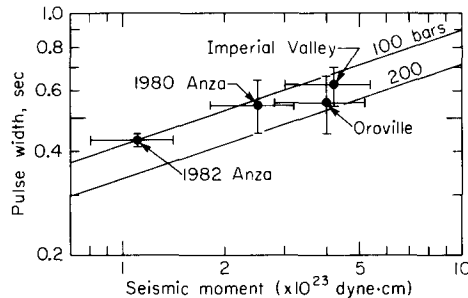


FIG. 8. Log of the average displacement pulse width plotted against the log of the seismic moment for the four earthquakes discussed in this paper. Error bars represent one standard deviation. Diagonal lines are lines of constant stress drop. Note that the stress drops of these four events range between about 100 and 200 bars.

response. In addition, some variation in pulse width between stations for a given event could be caused by source directivity. Without sufficient azimuthal coverage, however, the rupture geometry cannot be constrained well enough to correct the pulse widths.

Figure 8 also depicts the standard deviations calculated for the pulse widths and seismic moments. The standard deviations in pulse width are about 0.1 sec. Thus, the variation in the average pulse width between the 1980 event near Anza, the Imperial Valley aftershock and the Oroville aftershock is within one standard deviation. Additional error in the stress drop determination is produced by uncertainty in the seismic moment. For the strong-motion measurements of seismic moment, the standard deviations are about 25 per cent of the means. Scatter in the seismic moment values is caused by such factors as the local site conditions and errors in the radiation pattern corrections. The standard deviations in pulse width and seismic moment imply that the stress drop has an uncertainty of at least a factor of three.

The similarity of the stress drops for these earthquakes may indicate that the stress levels are comparable in the localized area near the hypocenters. Regional variations of stress may be secondary to the stress concentrations which occur at

asperities along a fault zone. For example, the Imperial Valley aftershock of 23:19 UTC occurred very close to an asperity that Hartzell and Heaton (1983) identified from strong-motion and teleseismic records of the main shock. Thus, the stress drop of this aftershock may be untypically high for events in the Imperial Valley.

However, Hartzell and Brune (1977) reported stress drops ranging from 10 to about 600 bars for events with moments between 10^{20} and 10^{22} dyne-cm that occurred near the Brawley fault in the Imperial Valley. These calculations were based on corner frequency and spectral amplitude measurements taken from waveforms recorded by a nearby SMA. Therefore, it is not uncommon for earthquakes in the Imperial Valley to have relatively high stress drops.

Frankel and Kanamori (1983) used local network data to estimate stress drops for 10 earthquakes of magnitude 3.5 to 3.9 in southern California. They reported a factor of ten difference in stress drop for two events only 1.5 km apart and occurring within 1 hr. These shocks occurred along the San Jacinto fault system just southeast of the 1980 earthquake discussed in this paper. This observation implies that the stress drops of these small events are providing information about localized stress concentrations rather than regional stress levels.

It is difficult to evaluate the results of this paper in terms of the likelihood of a moderate earthquake occurring in the Anza gap in the near future. More events need to be studied to ascertain whether the stress drops of the earthquakes discussed in this paper are representative of the earthquakes in each tectonic regime. One complication with the results presented here is that we have compared main shocks with aftershocks. Main shocks may have systematically different stress drops than aftershocks that occur in the same area. It is also possible that regional variations in stress drop may only be apparent in the averages of large numbers of events. Another important part of future efforts should be the incorporation of empirical path corrections, which may reduce somewhat the variance in pulse widths observed for $M_L \sim 5$ earthquakes. These path corrections can be derived by using the waveforms of adjacent small events ($M_L < 2$) as empirical Green's functions (Frankel and Kanamori, 1983).

ACKNOWLEDGMENTS

I thank Hiroo Kanamori, Steve Hartzell, and Terry Webb for reviewing the manuscript and providing helpful comments. Joe Fletcher, Gerry Brady, and Peter Mork of the U.S. Geological Survey kindly provided strong-motion records for the earthquakes near Anza. Doug Given provided the fault-plane solution for the 1982 Anza event. I benefitted from discussions with Jack Boatwright and Joe Fletcher. Comments from an anonymous reviewer were helpful in improving the manuscript. The figures were drafted by Laszlo Lenches. This research was supported by the U.S. Geological Survey under Grant 14-08-0001-21210. The author was supported by a Bantrell Postdoctoral Fellowship.

REFERENCES

- Aki, K. and P. G. Richards (1980). *Quantitative Seismology: Theory and Methods*, W. H. Freeman and Company, San Francisco, California.
- Archuleta, R. J., E. Cranswick, C. Mueller, and P. Spudich (1982). Source parameters of the 1980 Mammoth Lakes, California, earthquake sequence, *J. Geophys. Res.* **87**, 4595-4608.
- Ben-Menahem, A. (1962). Radiation of seismic body waves from a finite moving source in the earth, *J. Geophys. Res.* **67**, 345-350.
- Boatwright, J. (1980a). A spectral theory for circular seismic sources; simple estimates of source dimension, dynamic stress drop and radiated seismic energy, *Bull. Seism. Soc. Am.* **70**, 1-28.
- Boatwright, J. (1980b). Preliminary body-wave analysis of the St. Elias, Alaska earthquake of February 28, 1979, *Bull. Seism. Soc. Am.* **70**, 419-436.
- Brune, J. N. (1970). Tectonic stress and the spectra of seismic shear waves from earthquakes, *J. Geophys. Res.* **75**, 4997-5009.

- Combs, J. (1971). Heat flow and geothermal resource estimates for the Imperial Valley, in *Cooperative Geophysical-Geochemical Investigation of Geothermal Resources in the Imperial Valley Area of California*, Education Research Service, University of California, Riverside, California, 5-27.
- Corbett, E. J. and C. E. Johnson (1982). The Santa Barbara, California, earthquake of 13 August 1978, *Bull. Seism. Soc. Am.* **72**, 2201-2226.
- Fletcher, J. B., A. G. Brady, and T. C. Hanks (1980). Strong-motion accelerograms of the Oroville, California aftershocks: data processing and the aftershock of 0350 August 6, 1975, *Bull. Seism. Soc. Am.* **70**, 243-267.
- Frankel, A. and H. Kanamori (1983). Determination of rupture duration and stress drop for earthquakes in Southern California, *Bull. Seism. Soc. Am.* **72**, 1527-1551.
- Fuis, G. W., W. D. Mooney, J. H. Healy, G. A. McMechan, and W. J. Lutter (1982). Crustal structure of the Imperial Valley region in the Imperial Valley, California earthquake of October 15, 1979, *U.S. Geol. Surv. Profess. Paper 1254*, 25-49.
- Given, D. (1983). Seismicity and structure of the trifurcation in the San Jacinto fault zone, Southern California, *Master's Thesis*, California State University, Los Angeles, California, 73 pp.
- Hanks, T. C. and R. K. McGuire (1981). The character of high-frequency strong ground motion, *Bull. Seism. Soc. Am.* **71**, 2071-2096.
- Harkrider, D. G. (1964). Surface waves in multilayered elastic media. Part I. Rayleigh and Love waves from buried sources in a multilayered elastic halfspace, *Bull. Seism. Soc. Am.* **54**, 627-679.
- Harkrider, D. G. (1970). Surface waves in multilayered elastic media. Part II, Higher mode spectra and spectral ratios from point sources in plane layered earth models, *Bull. Seism. Soc. Am.* **60**, 1937-1987.
- Hartzell, S. H. and J. N. Brune (1977). Source parameters for the January 1975 Brawley-Imperial Valley earthquake swarm, *Pageoph* **115**, 333-355.
- Hartzell, S. H. and J. N. Brune (1979). The Horse Canyon earthquake of August 2, 1975—two-stage stress release process in a strike-slip earthquake, *Bull. Seism. Soc. Am.* **69**, 1161-1174.
- Hartzell, S. H. and D. V. Helmberger (1982). Strong-motion modeling of the Imperial Valley Earthquake of 1979, *Bull. Seism. Soc. Am.* **72**, 571-596.
- Hartzell, S. H. and T. H. Heaton (1983). Inversion of strong ground motion and teleseismic waveform data for the fault rupture history of the 1979 Imperial Valley, California earthquake, *Bull. Seism. Soc. Am.* **73**, 1553-1584.
- Henye, T. L. and G. J. Wasserburg (1971). Heat flow near major strike-slip faults in California, *J. Geophys. Res.* **76**, 7924-7946.
- Liu, H.-L. (1983). Interpretation of near-source ground motion and implications, *Ph.D. Thesis*, California Institute of Technology, Pasadena, California, 184 pp.
- Madariaga, R. (1976). Dynamics of an expanding circular fault, *Bull. Seism. Soc. Am.* **66**, 639-666.
- Nigam, N. C. and P. C. Jennings (1968). Digital calculation of response spectra from strong-motion earthquake records. Report from the Earthquake Engineering Research Laboratory, California Institute of Technology, Pasadena, California, 65 pp.
- Sanders, C. O. and H. Kanamori (1984). A seismotectonic analysis of the Anza seismic gap, San Jacinto fault zone, Southern California, *J. Geophys. Res.* **89**, 5873-5890.
- Thatcher, W. and T. C. Hanks (1973). Source parameters of southern California earthquakes, *J. Geophys. Res.* **78**, 8547-8575.
- Thatcher, W., J. A. Hileman, and T. C. Hanks (1975). Seismic slip distribution along the San Jacinto fault zone, Southern California and its implications, *Geol. Soc. Am. Bull.* **86**, 1140-1146.
- Wallace, T. C., D. V. Helmberger, and J. E. Ebel (1981). A broadband study of the 13 August 1978 Santa Barbara earthquake, *Bull. Seism. Soc. Am.* **71**, 1701-1718.

SEISMOLOGICAL LABORATORY
 CALIFORNIA INSTITUTE OF TECHNOLOGY
 PASADENA, CALIFORNIA 91125
 CONTRIBUTION NO. 4066

Manuscript received 16 March 1984